Branching of hydraulic cracks enabling permeability of gas or oil shale with closed natural fractures

Saeed Rahimi-Aghdam[a], Viet-Tuan Chau[b], Hyunjin Lee[a], Hoang Nguyen[a], Weixin Li[a], Satish Karra[b], Esteban Rougier[b], Hari Viswanathan[b], Gowri Srinivasan[c], and Zdeněk P. Bažant[a,d,e,1]

[a]Department of Civil and Environmental Engineering, Northwestern University, Evanston, IL 60208; [b]Earth and Environmental Sciences Division, Los Alamos National Laboratory, Los Alamos, NM 87545; [c]X Computational Physics Division, Los Alamos National Laboratory, Los Alamos, NM 87545; [d]Department of Mechanical Engineering, Northwestern University, Evanston, IL 60208; and [e]Department of Materials Science, Northwestern University, Evanston, IL 60208

Contributed by Zdeněk P. Bažant, November 21, 2018 (sent for review October 29, 2018; reviewed by Huajian Gao and John Hutchinson)

While hydraulic fracturing technology, aka fracking (or fraccing, frac), has become highly developed and astonishingly successful, a consistent formulation of the associated fracture mechanics that would not conflict with some observations is still unavailable. It is attempted here. Classical fracture mechanics, as well as current commercial software, predict vertical cracks to propagate without branching from the perforations of the horizontal well casing, which are typically spaced at 10 m or more. However, to explain the gas production rate at the wellhead, the crack spacing would have to be only about 0.1 m, which would increase the overall gas permeability of shale mass about 10,000×. This permeability increase has generally been attributed to a preexisting system of orthogonal natural cracks, whose spacing is about 0.1 m. However, their average age is about 100 million years, and a recent analysis indicated that these cracks must have been completely closed by secondary creep of shale in less than a million years. Here it is considered that the tectonic events that produced the natural cracks in shale must have also created weak layers with nanocracking or microcracking damage. It is numerically demonstrated that seepage forces and a greatly enhanced permeability along the weak layers, with a greatly increased transverse Biot coefficient, must cause the fracking to engender lateral branching and the opening of hydraulic cracks along the weak layers, even if these cracks are initially almost closed. A finite element crack band model, based on a recently developed anisotropic spherocylindrical microplane constitutive law, demonstrates these findings [Rahimi-Aghdam S, et al. (2018) arXiv:1212.11023].

fracking | poromechanics | Biot coefficient | seepage forces | damage

Significant advances have been made in fracture mechanics of propagation of a single hydraulic crack in elastic rock under tectonic stress (1–11). They include characterization of the stress singularity at the tip of a water-filled advancing crack; flow of water of controlled viscosity along the crack, with or without proppant grains; and water leak-off into the shale. Interactions of parallel cracks, their stability, closing, and stress shadow effect have also been clarified (12–15). Discrete element models, in which the hydraulic crack was simulated by a band of interelement separations (16, 17), led to similar results.

These studies, however, predicted no branching of the hydraulic cracks, originally spaced at cca 10 m. This presented a dilemma since branching is the only way to reduce the crack spacing to about 0.1 m, which is necessary to explain the gas production rate. Consequently, it has been universally hypothesized that the preexisting natural cracks, spaced at *ca.* 0.1 m, would somehow increase the overall permeability of the shale mass. A 10,000-fold increase of permeability would be necessary to match the gas production rate. However, recent analysis (18, 19) showed that the natural, tectonically produced, cracks, which are, on the average, about 10^8 years old, must have been closed by secondary creep (or viscous flow) of shale under tectonic stress within 10^4 years to 10^6 years (if not filled earlier by calcite deposit). This invalidated the hypothesis.

It might be objected that water in the cracks could have prevented crack closing. However, the open spaces in shear cracks, created (due to shear dilatancy) by a tectonic event, could not have been filled by water immediately. If the water had to seep in from the ground surface, it would take about 10 million years and, if from a nearby water-filled rock formation, certainly over a million years. This must have left plenty of time for the creep closing to proceed uninhibited.

A recent paper (20) presented a new model which, by contrast with all of the previous studies, took into account (*i*) the seepage forces (i.e., the body forces due gradients of pore pressure in Darcy diffusion of water into porous shale) and (*ii*) the variation of effective Biot coefficient for the water pressure on the crack plane, caused by gradually vanishing bridges between the opposite faces of a widening bridged crack (another difference from the previous studies was abandoning the assumption of incompressibility of water in the cracks, since water is about 20 times more compressible than shale). This model (20) did predict extensive lateral crack branching.

Later analysis, however, showed that the branching indicated by the computer program in ref. 20 was, in fact, triggered by the unintended coding of a sudden change of Biot coefficient for transverse water pressure on the crack. This change abruptly increased the water pressure on the solid phase and triggered dynamic response. Such a sudden trigger is probably unrealistic, which represents a vital correction to the preceding study (20) (this correction nevertheless reveals a useful fact, namely, that fluid pressure shocks could greatly enhance crack branching).

If Biot coefficient is changed gradually, the model from the previous study (20) would predict no crack branching, although the branching must occur to explain the observed gas production rate. This study will show that, if the previous model (20) is enhanced by introducing, into the shale mass, significant heterogeneity due to damaged weak layers along preexisting natural cracks, then an extensive and dense crack branching is predicted.

It may be noted that the fracking companies are aware of the necessity of branched cracks running along preexisting natural fractures. Fig. 1 shows a picture similar to what is found on the websites of some companies. However, this awareness seems to be merely intuitive and empirical. The existing commercial software, as well as fracture mechanics studies, predicts

Significance

Development of a realistic model of fracking would allow better control. It should make it possible to optimize various parameters such as the history of pumping, its rate or cycles, changes of viscosity, etc. This could lead to an increase of the percentage of gas extraction from the deep shale strata, which currently stands at about 5% and rarely exceeds 15%.

Author contributions: S.R.-A. and Z.P.B. designed research and conceived the mathematical model; S.R.-A., V.-T.C., H.L., H.N., W.L., S.K., E.R., H.V., G.S., and Z.P.B. performed research; S.R.-A. analyzed data; and S.R.-A. and Z.P.B. directed the research and wrote the paper.

Reviewers: H.G., Brown University; and J.H., Harvard University.

The authors declare no conflict of interest.

[1]To whom correspondence should be addressed. Email: z-bazant@northwestern.edu.

Published online January 11, 2019.

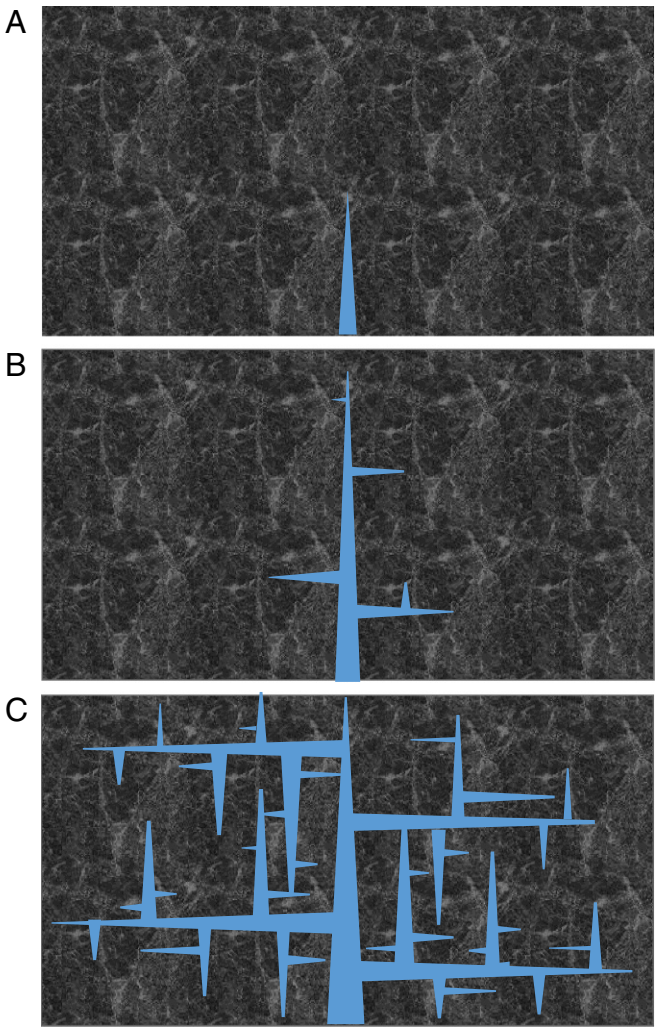

Fig. 1. Schematic branching due to natural fractures. (*A*) Water is injected at high pressure through damaged zones and weak layers, (*B*) crack branching initiates due to the presence of damaged zones and natural fractures, and (*C*) dense cracking happens in all directions, due to the presence of damaged zones, weak layers at closed natural fractures (downward view normal to bedding plane).

no branching. So an intersecting system of open natural fractures is assumed to either exist a priori or to develop according to some empirical criteria with no basis in mechanics, supported by some recent experiments indicating the possibility of branching (21–24). A physics-based model for branching, which is our goal, seems lacking.

Fluid Flow in Porous Solid, Without or With Cracking Damage

Two types of flow play a role in hydraulic fracturing: (*i*) the flow along the hydraulically created cracks, typically a few millimeters wide, and (*ii*) the flow through nanoscale pores and microcracks or nanocracks in shale with preexisting damage. The latter is negligible after continuous hydraulic cracks form, but here it is found to be crucially important for crack initiation and branching. The volume flow, $\boldsymbol{q}$, of water through the pores and nanocracks or microcracks of isotropic material may be approximately calculated from the Darcy law: $\boldsymbol{q} = -(K/\mu)\boldsymbol{\nabla}\psi$, where K is the permeability, μ is the dynamic viscosity, and ψ is the phase potential calculated as $\psi = p - \gamma_g z$. Here p is the pore pressure, γ_g is the pressure gradient due to gravity, and z is the depth from a datum. However, the permeability K_v in the direction normal to the bedding planes (x, y), i.e., in vertical direction z, is much lower than permeability K_h along these planes (horizontal). Therefore, the 3D Darcy law is, in general, anisotropic. In Cartesian coordinates (x, y, z), the resulting volume flux vector $\boldsymbol{q} = (q_x, q_y, q_z)$ may be written as

$$\boldsymbol{q} = -\mu^{-1}\boldsymbol{K}\cdot\boldsymbol{\nabla}\psi, \qquad [1]$$

where $\boldsymbol{\nabla}$ is the vector of gradient operator; $\boldsymbol{K}$ is the 3×3 permeability matrix, which is diagonal if (and only if) the Cartesian axes x, y, z are chosen to be parallel and normal to the bedding planes.

Although the natural (or preexisting) cracks in shale strata at 3 km depth must have been closed by 100 million years of creep, the damage bands along these cracks, which always accompany propagation of fracture process zone, certainly remain (in fact, based on the known surface energy of shale, it can be shown that even empty pores and cracks *ca.* <15 nm in size, at depth 3 km, cannot close, and this is confirmed by the known size of pores containing shale gas). Permeability K_{xx} along these bands is surely much higher than it is in the intact shale (although pores of <15 nm contribute nothing globally).

To prevent the formation of horizontal cracks, the pumping pressure is assumed not to exceed the overburden pressure, which is about 75 MPa. Hydraulic fracturing is considered to produce a system of mutually orthogonal vertical cracks, normal to the directions of the minimum and maximum principal tectonic stresses. The flow of the second type, along the hydraulically created cracks, may be assumed to follow the Reynolds equations of classical lubrication theory, which are based on the Poiseuille law for viscous flow. Thus, the horizontal and vertical flow vector components in x, y, z directions along with the cracks may be calculated as

$$Q_x = -\frac{h_y^2}{12\,\mu}\nabla_x p, \quad Q_y = -\frac{h_x^2}{12\,\mu}\nabla_y p, \quad Q_z = -\frac{h_x^2 + h_y^2}{12\,\mu}\nabla_z p, \qquad [2]$$

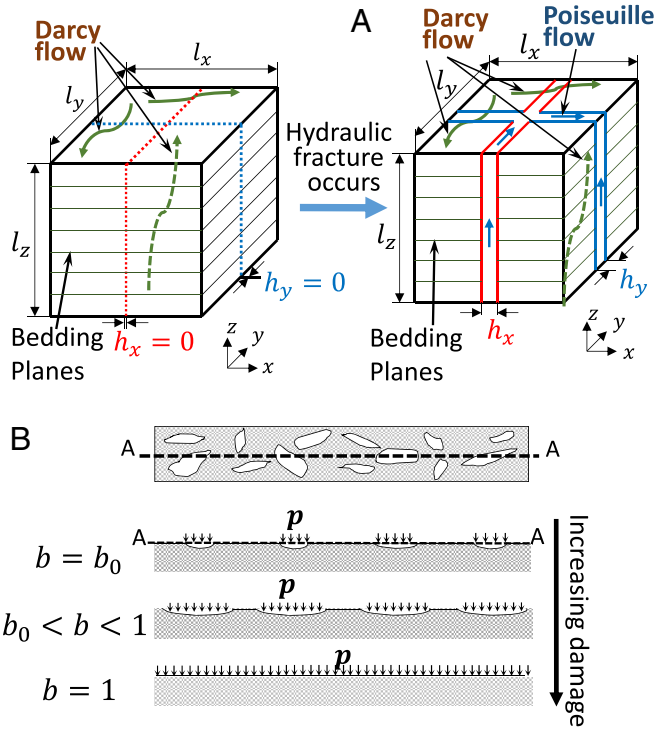

Fig. 2. (*A*) Fluid flow in intact and damaged shale. (*B*) Biot coefficient increase in transverse direction due to increasing damage (20).

where $\nabla_x = \partial/\partial_x, \ldots$; h_x, h_y are the opening widths of vertical cracks normal to axes x and y that are positioned into the bedding plane.

An effective way to simulate the hydraulic cracks numerically is the crack band model (25–27), in which cracking deformation is considered smeared over the band (or element) width. The widths of cracks normal to x and y are (Fig. 2)

$$h_x = l_x \epsilon''_{xx}, \quad h_y = l_y \epsilon''_{yy}, \qquad [3]$$

where $\epsilon''_{xx}, \epsilon''_{yy}$ are damage parts of normal strains due to smeared cracking normal to x and y directions; l_x, l_y are the widths of crack bands, assumed equal to the minimum possible spacing of adjacent parallel hydraulic cracks (l_x, l_y must be treated as a material property, related to fracture energy G_f of shale; here l_x, l_y are not changed but, if they were, the postpeak softening would have to be adjusted to preserve G_f). Furthermore,

$$\epsilon''_{ij} = \epsilon_{ij} - \epsilon^{el}_{ij}, \quad \epsilon^{el}_{ij} = C_{ijkl}\sigma_{kl}, \qquad [4]$$

where C_{ijkl} is the transversely isotropic elastic compliance tensor of shale (for unloading); $\sigma_{ij}, \epsilon_{ij}$ are the stress and strain tensors in the rock, calculated from a constitutive model for smeared cracking damage [with a localization limiter (25)], for which the spherocylindrical microplane constitutive model (28) has been used. The coordinates are Cartesian, $x_i, i = 1, 2, 3$ ($x_1 \equiv x, x_2 \equiv y, x_3 \equiv z$). Note that, the same as in ref. 20, water is considered as compressible. It is, in fact, about 20 times more compressible than concrete, and the water pressure during fracking can be high (up to 70 MPa).

Equilibrium in Two-Phase Solid and Biot Coefficient

The shale may be modeled as a two-phase medium with water-saturated pores, for which the classical Biot-type relations for the equilibrium of the phases apply. For undamaged shale, they read

$$S_{ij} = \sigma_{ij} - \delta_{ij} b_0 p, \qquad [5]$$

where p is the pore pressure, b_0 is the Biot coefficient of undamaged shale, S_{ij} is the total stress tensor, σ_{ij} is the stress tensor in the solid phase, and δ_{ij} is the Kronecker delta. As a special case, $S_V = \sigma_V - b_0 p$, where $S_V = S_{kk}/3$ is the volumetric total stress, and $\sigma_{ij} = \sigma_{kk}/3$ is the volumetric stress in the solid phase.

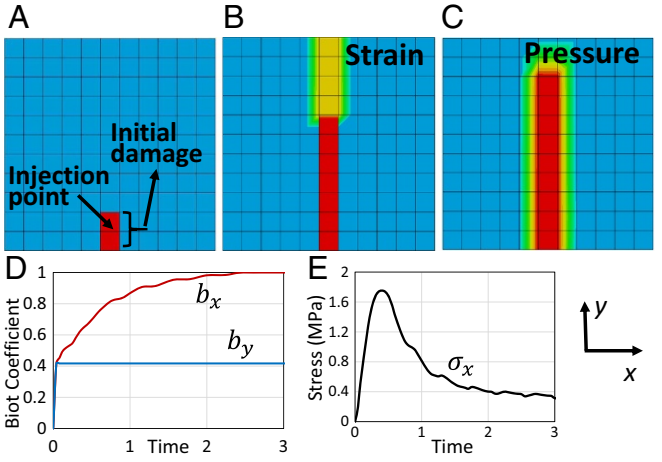

Fig. 3. Results of two-phase FE simulations in case of a single damage band. (*A*) Initial model. (*B*) Strain ϵ_{xx} due to water injection (the red marks the highest values; the blue marks the smallest values). (*C*) Pressure propagation. (*D*) Stress evolution vs. injection time for the first element above the initially damaged elements. (*E*) Evolution, along the damage band, of the Biot coefficient transverse to the band.

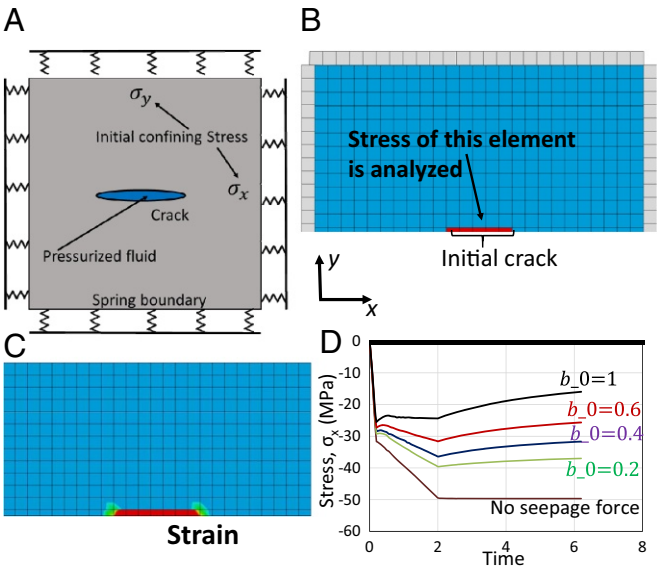

Fig. 4. (*A*) Pressurized line crack in a 2D domain of a two-phase porous solid (shale) supported by springs at boundaries, subjected to tectonic stresses T_x and T_y. (*B*) FE mesh for one-half of the domain. (*C*) Extension of the band of high strain. (*D*) Evolution of stress σ_{xx} in solid part in the element at the center of initial crack face.

While, typically, $\varphi = 0.1$, the Biot coefficient of shales can vary between 0.2 and 0.7. Test results (29–34) show that it increases with the cracking damage and depends on the load direction. This requires generalizing the Biot coefficient as a tensor, b_{ij} (35). The following, tensorially consistent, empirical relation, which appears to match test data, is proposed:

$$b_{ij} = \min\left\{b_0 + \beta\epsilon''_{ij}(\epsilon''_{kk}/3)^{-2/3},\ 1\right\} \quad (\varphi \le b_0 \le 1). \qquad [6]$$

Here b_0 refers to undamaged material, β is an empirical parameter, ϵ''_{ij} is the inelastic damage strain tensor, and φ is the natural porosity of shale. For the Biot coefficient in the direction of unit vector ν_i, this equation gives $b_\nu = \nu_i\nu_j b_{ij} = b_0 + \beta\epsilon''_\nu(\epsilon''_V)^{-2/3}$ (but ≤ 1), where $\epsilon''_V = \epsilon''_{kk}/3$ is the inelastic relative volume expansion, and $\epsilon''_\nu = \nu_i\nu_j\epsilon''_{ij}$ is the inelastic normal strain component in direction of vector ν_i.

For the special case of microcracking or nanocracking normal to x_1 direction only, one has $\epsilon''_V = \epsilon''_{11}/3$ and $b_\nu = b_0 + \beta(9\epsilon''_{11})^{1/3}$ (but ≤ 1). This equation can be interpreted graphically as seen in Fig. 2*B*, which shows section A–A of a band of preexisting, mostly aligned, microcracks and the compressive stresses applied by the pore fluid onto the microcrack faces, resisted by tensile stresses in the ligaments of the solid between the microcrack tips.

The viscous drag of water flowing through a soil imposes a seepage force on the soil in the direction of flow. The seepage forces are body forces defined as

$$\boldsymbol{f}_s = -b\nabla p. \qquad [7]$$

The seepage forces are applied on the porous solid and must be balanced by stresses in the solid. Seepage in an upward direction reduces the effective stress within the soil. When the water pressure at a point in the soil is equal to the total vertical stress at that point, the effective stress is zero, and the soil has no frictional resistance to deformation (36, 37). The seepage force have long been considered in geotechnical engineering to assess the risk of sand liquefaction in cofferdams (38, 39) or under dams. However (except for ref. 20), they have been ignored in previous studies of hydraulic fracturing, although they do play a crucial role in crack branching. A poromechanical finite element (FE) code for a

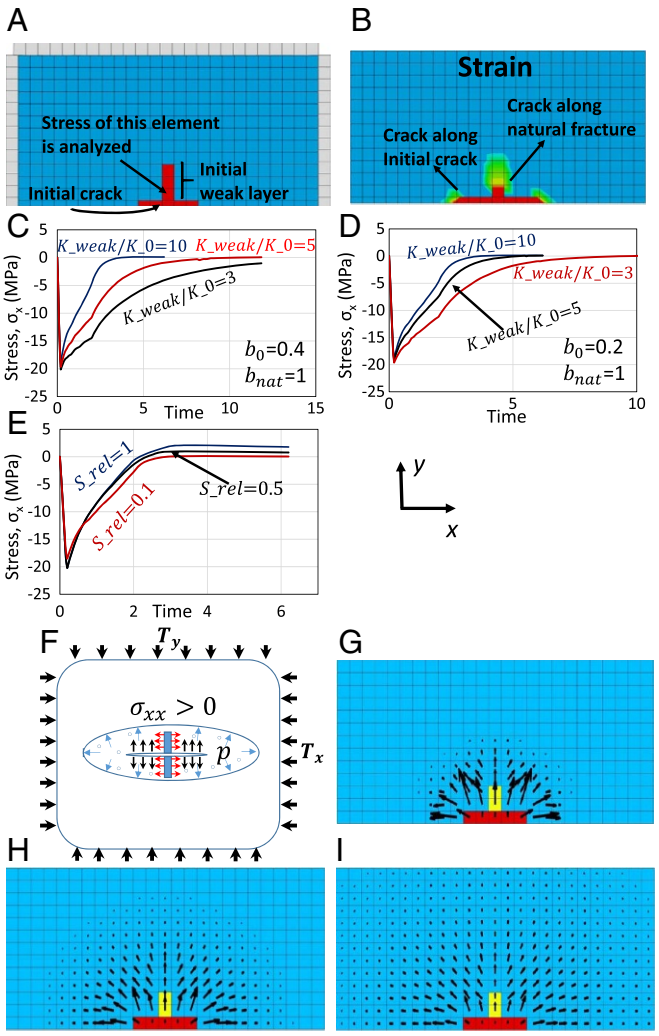

Fig. 5. (*A*) Schematic line crack with weak layer and spring boundaries. (*B*) Strain and damage evolution. (*C*) Stress in solid part of one element in weak layer for a shale with $b_0 = 0.4$ and different weak layer permeabilities. (*D*) Stress in solid part of one element in weak layer for $b_0 = 0.2$ and different weak layer permeabilities. (*E*) Stress in solid part of one element in weak layer for $b_0 = 0.4$ and different relative weak layer strengths. (*F*) Schematic of seepage forces. (*G–I*) Evolution of seepage forces.

two-phase solid automatically takes the seepage forces into account in the form of nodal forces.

Two-Phase FE Simulations for a Single Damage Band

To clarify the role of nanocracking or microcracking, consider first a horizontal 2D square block of shale of dimensions 1.1 m × 1.1 m, supported at the sides by springs approximately equivalent to an infinite medium, as shown in Fig. 3*A*. Water is injected at the center of the south side at the constant rate of 2 m^3/s. The anisotropic spherocylindrical microplane model, with the default parameters of shale given in ref. 28, is used as the constitutive model; $l_x = l_y$ = 2.1 m. The initial Biot coefficient is $b_0 = 0.4$. The tectonic stresses are $T_x = -30$ MPa and $T_y = -30$ MPa.

Consider that there is a single preexisting band of nanocracks or microcracks predominantly aligned with axis y, represented by the two red elements in Fig. 3*A* (which is what remains after a crack was closed by up to a million years of secondary creep, or viscous flow of rock). These cracks cause the vertical permeability in these two elements to increase *ca*. 1,000 times compared with undamaged shale, while the Biot coefficient increases up to 1 and the initial strength decreases to 10% of intact shale.

Fig. 3 *B* and *C* shows how damage and pressure propagate after water injection. For this case, the crack band with high water pressure is seen to propagate straight forward, without branching. Now look at stress variation. Fig. 3*D* shows the stress evolution within in the solid part of the first element above the initial damaged elements. Obviously, the damage during post-peak softening is captured in a stable manner. Finally, consider how the Biot coefficient and permeability vary in one cracked element (the first above the initial damaged elements). Fig. 3*E* contrasts the evolution of Biot coefficient in the transverse direction with its constancy in the forward direction, which agrees with experimental observations.

Do the Seepage Forces Suffice to Induce Crack Branching?

It is well known in classical fracture mechanics that pressurizing a crack cannot produce tension along the crack faces, and thus cannot initiate lateral crack branching (branching is possible only at the tip of a crack propagating at nearly the Raleigh wave speed). In a preceding study (20), it was surmised, under various simplifications, that the seepage forces (Eq. **7**) would suffice to produce tension along the crack face and thus initiate lateral crack branching. Let us examine this more rigorously. Consider again a horizontal 2D square domain 2.5 m × 2.5 m, containing one line crack (Fig. 4*A*). By virtue of symmetry, only a half-domain is simulated (Fig. 4*B*). The water pressure in the line crack is gradually ramped up to reach the maximum of

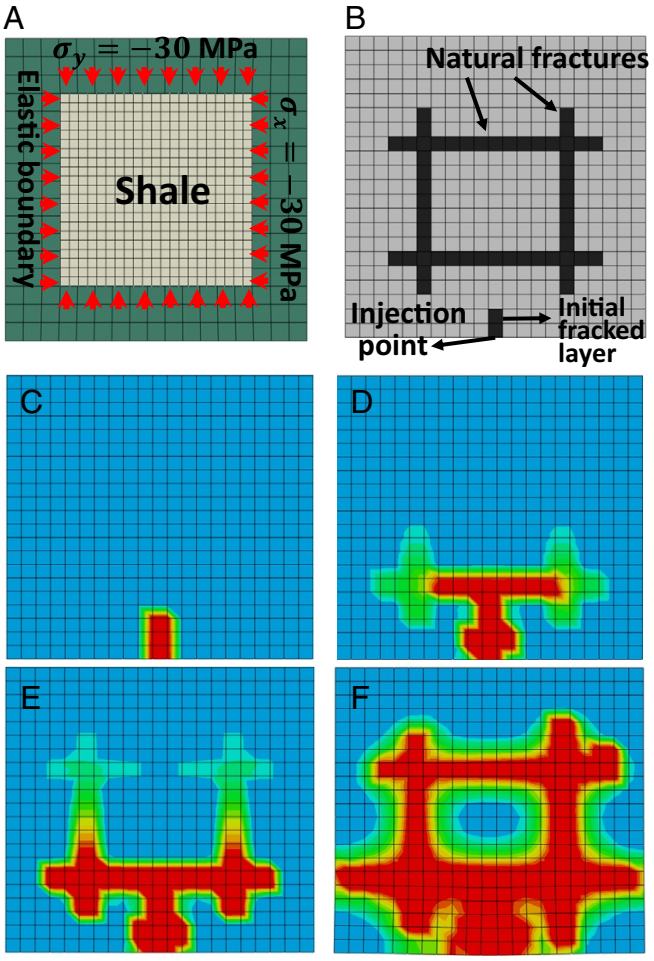

Fig. 6. FE simulation of hydraulic crack branching in a small domain of shale with several orthogonal weak layers along perfectly closed natural fractures. (*A*) Ring of elastic elements providing elastic support of the boundaries. (*B*) FE mesh, preexisting natural weak layers, and fracking water inlet. (*C–F*) Evolution of pressure in a shale with weak layers.

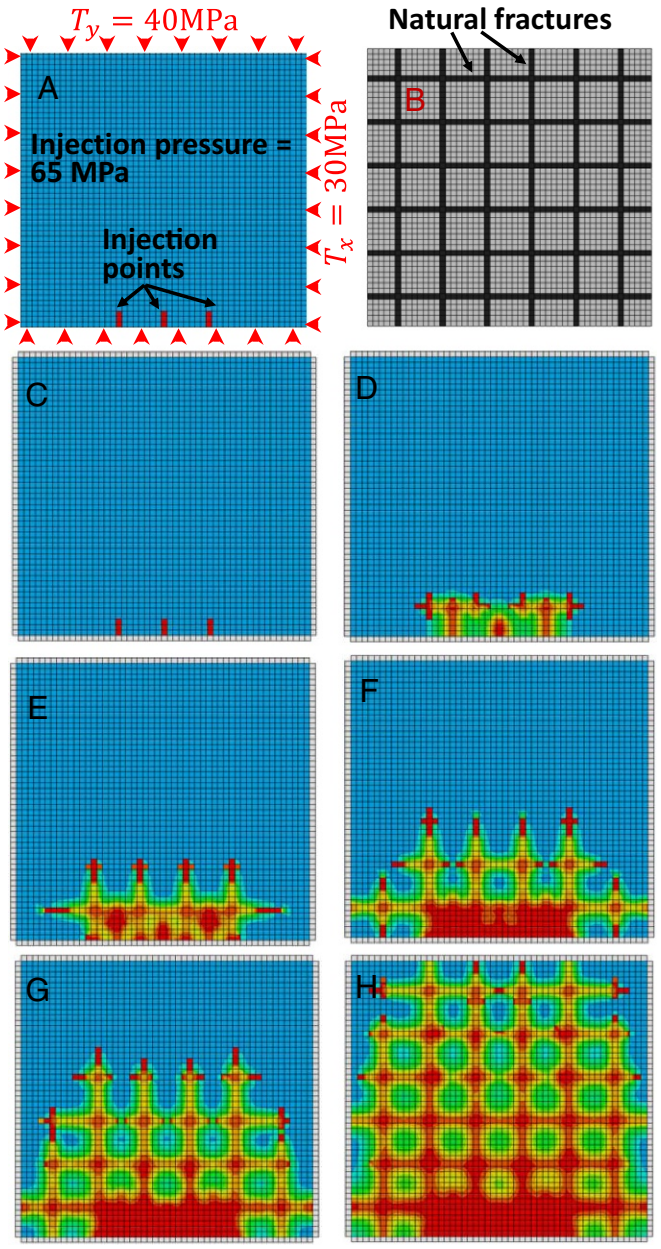

Fig. 7. The 2D FE simulation of fracking process in a horizontal domain with a larger system of natural fractures or weak layers (the red zone shows the propagation of high water pressure). (*A*) FE mesh, injection points, and boundaries. (*B*) Orthogonal system of preexisting natural fractures. (*C–H*) Evolution of pressure in a shale with weak layers and initially closed natural fractures.

50 MPa. Water diffusion from the pressurized crack into the shale is simulated via Darcy law. First, we neglect the increase of Biot coefficient due to damage ($\beta = 0$). Fig. 4*C* shows that the damage, as well as the crack, propagates only in the direct extension of the initial line crack, i.e., there is no branching. Fig. 4*D* shows the evolution of stress in the solid part, σ_{xx}, along the crack face. The results show that the Biot coefficient can have a major effect and cannot be ignored.

Lateral crack branching would happen if the stress in the solid phase became positive (tensile) and attained the tensile strength of shale. The results show that this cannot happen, regardless of the tectonic stress value (even if vanishing). Nevertheless, the seepage forces are seen to reduce the magnitude of compressive stress along the crack face significantly.

We must thus conclude (as an update of ref. 18) that the seepage forces alone do not suffice to explain and model lateral branching of hydraulic cracks. So, what additional phenomena could explain the lateral branching? Not surprisingly, the explanation is the natural (preexisting) fractures, even though they must have been completely closed due to millions of years of secondary creep, or flow. We demonstrate it next.

Hydraulic Crack Branching in Two-Phase Porous Solid with Closed Natural Fractures

In Fig. 5*A*, we now consider the same 2D domain of two-phase porous solid as before, except that now there are two natural weak layers (or preexisting damage bands) in both x and y directions. The crack is uniformly pressurized, and water diffuses out. The transverse Biot coefficient within the weak layers that represent the closed natural fractures is $b_{nat} = 1$, because the weak layer (or natural fracture) may consist of separate original crack faces in contact (uncemented by limestone deposit), while, in the intact shale, the b_{ij} values increase according to Eq. **6** from the initial value $b_0 = 0.4$ (Fig. 5*C*) or 0.2 (Fig. 5*D*).

Fig. 5*B* reveals that the hydraulic crack tends to propagate simultaneously along the initial crack and along the weak layer. This confirms that branching can occur if transverse weak layers exist. Further, consider the normal stress parallel to the crack in one element of the weak layer. If this stress attains the tensile strength, a lateral crack branch can initiate, and shale branching can happen. Fig. 5*B* shows the spreading of high and lower transverse strains along both weak layers for the case of Biot coefficient $b = 0.4$, with permeability K_{weak} along the weak band 5 times bigger than K_0 for intact shale.

The computed effect of ratio K_{weak}/K_0 on the σ_{xx} evolution in the first element of the weak layer above initial crack is plotted in Fig. 5 *C* and *D* for the initial Biot coefficients, $b_0 = 0.4$ and 0.2. As water diffuses into the shale, the stress in the weak layer increases from negative to tensile values until it finally reaches the tensile strength of the weak layer. Evidently, a greater difference in Biot coefficient between the weak layer and the shale facilitates, and speeds up, the crack branching.

Finally, to clarify the effect of the transverse tensile strength of the weak layer, three relative strength S_{rel} values are considered in Fig. 5*E* (here S_{rel} is the damaged-to-intact strength ratio of shale). As seen, a smaller S_{rel} leads to smaller stress, but, generally, the effect of S_{rel} is almost negligible. Hence, whether or not the natural cracks are cemented by limestone is almost irrelevant.

It is instructive to see the evolution of the seepage force vectors acting on the mesh nodes, as portrayed in Fig. 5. Fig. 5*F* shows schematically the seepage forces acting on an ellipse around the crack. Fig. 5 *G–I* illustrates the evolution of seepage forces. Their orientations make it intuitively clear that they must produce a biaxial tension in the porous solid at the center of the pressurized domain.

From all these observations, it transpires that a major stimulus for crack branching is the difference in the Biot coefficient and in the permeability between the weak layers and the intact shale, as well as the shale mass heterogeneity due to the alternation of weak layers and intact porous solid.

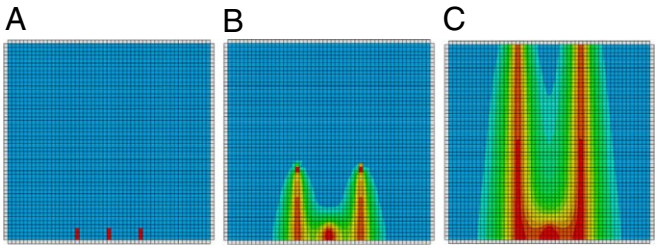

Fig. 8. (*A–C*) Water pressure propagation for no weak layers, no natural fractures.

It is worth mentioning that the expansion of solid due to the effect of Biot coefficient has been thought to prevent any tension parallel to the crack face, and thus cause the closing of any lateral crack. The preceding results show that this skeptical view does not extend to a heterogeneous shale mass containing weak layers alternating with intact shale.

Next consider the horizontal section in Fig. 6*A*, with 4 weak layers; $b_{weak} = 1$, $S_{rel} = 0.1$, $K_{weak}/K_0 = 1000$ (Fig. 6*B*). Water is injected at one point at constant flow rate. Fig. 6 *C–E* the propagation of high water pressure. Water enters through prefractured elements, then diffuses along the weak layers and, upon attaining sufficient pressure, the crack branches and Poiseuille flow dominates. The importance of weak layers is thus evidenced.

To demonstrate the present theory on a larger scale, consider a bigger horizontal section of shale, a square domain 5 m × 5 m, containing a uniform orthogonal system of closed natural fractures with aligned preexisting weak layers (Fig. 7). To be more realistic, unequal tectonic stresses are considered in x and y directions; T_x= 30 MPa, and T_y = 40 MPa.

Water is injected at three points at the bottom of Fig. 7*A*. Fig. 7 *C–H* shows the evolution of water pressure. The water flow and damage strain are seen to follow the path of weak layers. Extensive branching occurs. Obviously, this branching can create closely spaced hydraulic cracks and thus increase the overall permeability of shale stratum by orders of magnitude, compared with nonbranching cracks in intact shale.

It has also been checked that omitting the natural fractures leads to no branching. This is evident from the pressure propagation pattern in Fig. 8. This figure also documents the localization instability of parallel crack system (12) (also known as the stress shadow effect), which causes the crack emanating from the middle injection point not to grow long (the long simultaneous growth of both remaining cracks is made possible by the proximity of the boundaries).

Conclusions

i) The natural fractures have a major effect on hydraulic fracturing and are crucial for its success (although they are currently neglected by commercial software).

ii) Even though the natural fractures must have been closed by millions of years of creep, or sealed by mineral deposits, a weak layer of nanocracks and microcracks along these fractures must be expected to facilitate water diffusion.

iii) Poromechanics with Biot coefficient depending on the damage of the solid phase must be used in fracking analysis.

iv) Increase of the Biot coefficient in the transverse direction, caused by oriented cracking damage inflicted by fracking, is essential to achieve crack branching.

v) The typical spacing between natural fractures is roughly 0.1 m. This matches the hydraulic crack spacing that is necessary to explain the typical gas production rate at the wellhead.

vi) The widespread opinion that preexisting natural fractures somehow explain why the overall permeability of shale mass, inferred from the gas production rate, appears to be about 10,000 times higher than what is measured on shale cores in the laboratory has been basically correct. However, these fractures are completely closed and do not convey any gas, and their role is indirect.

vii) (*i*) No porosity ⇒ no branching. (*ii*) No seepage forces ⇒ no branching. (*iii*) No weak layers ⇒ no branching. (*iv*) Constant Biot coefficient ⇒ no branching. (Note that, consequently, hydraulic crack branching in granite is impossible.)

ACKNOWLEDGMENTS. Z.P.B. thanks Emmanuel Detournay for valuable discussions and a stimulating challenge that provoked part of this study. The work at Northwestern was funded by Los Alamos National Laboratory (Grants DOE LDRD 20170103DR and OBES DE-AC52-06NA25396) to Northwestern University. Z.P.B. is McCormick Institute Professor and W. P. Murphy Professor of Civil and Mechanical Engineering and Materials Science at Northwestern University.

1. Abe H, Keer LM, Mura T (1976) Growth rate of a penny-shaped crack in hydraulic fracturing of rocks, 2. *J Geophys Res* 81:6292–6298.
2. Beckwith R, et al. (2010) Hydraulic fracturing: The fuss, the facts, the future. *J Pet Technol* 62:34–40.
3. Adachi JI, Detournay E (2008) Plane strain propagation of a hydraulic fracture in a permeable rock. *Eng Fract Mech* 75:4666–4694.
4. Advani SH, Torok JS, Lee JK, Choudhry S (1987) Explicit time-dependent solutions and numerical evaluations for penny-shaped hydraulic fracture models. *J Geophys Res Solid Earth* 92:8049–8055.
5. Carbonell RS (1997) Self-similar solution of a fluid-driven fracture. PhD thesis (Univ Minnesota, Minneapolis).
6. Detournay E, Garagash DI (2003) The near-tip region of a fluid-driven fracture propagating in a permeable elastic solid. *J Fluid Mech* 494:1–32.
7. Adachi JI (2002) Fluid-driven fracture in permeable rock. PhD thesis (Univ Minnesota, Minneapolis).
8. Peter V, Economides MJ (1995) *Hydraulic Fracture Mechanics* (Wiley, New York).
9. Zoback MD (2010) *Reservoir Geomechanics* (Cambridge Univ Press, Cambridge, UK).
10. Detournay E (2016) Mechanics of hydraulic fractures. *Annu Rev Fluid Mech* 48:311–339.
11. Detournay E (2004) Propagation regimes of fluid-driven fractures in impermeable rocks. *Int J Geomech* 4:35–45.
12. Bažant ZP, Oh BH (1985) Microplane model for progressive fracture of concrete and rock. *J Eng Mech* 111:559–582.
13. Bažant ZP, Salviato M, Chau VT, Viswanathan H, Zubelewicz A (2014) Why fracking works. *J Appl Mech* 81:101010.
14. Bunger AP, Detournay E, Garagash DI (2005) Toughness-dominated hydraulic fracture with leak-off. *Int J Fract* 134:175–190.
15. Bunger AP, Cardella DJ (2015) Spatial distribution of production in a marcellus shale well: Evidence for hydraulic fracture stress interaction. *J Pet Sci Eng* 133:162–166.
16. Schlumberger (2012) *Fraccade* (Schlumberger, Houston).
17. NSI Technologies (2014) *Stimplan* (NSI Technol, Tulsa, OK), Version 7.0.
18. Chau VT, Li C, Rahimi-Aghdam S, Bažant ZP (2017) The enigma of large-scale permeability of gas shale: Pre-existing or frac-induced?. *J Appl Mech* 84:061008.
19. Bažant ZP, Chau VT, Rahimi-Aghdam S (2017) Three-phase cracked porous medium: Shale fracking and ASR damage. *Poromechanics VI* (Am Soc Civ Eng, Reston, VA), pp 1–8.
20. Chau VT, Bažant ZP, Su Y (2016) Growth model for large branched three-dimensional hydraulic crack system in gas or oil shale. *Phil Trans R Soc A* 374:20150418.
21. Weng X, Kresse O, Cohen CE, Wu R, Gu H (2011) Modeling of hydraulic fracture network propagation in a naturally fractured formation. *Proceedings of the SPE Hydraulic Fracturing Technology Conference* (Soc Petrol Eng, Pittsburgh).
22. Blanton TL, et al. (1982) An experimental study of interaction between hydraulically induced and pre-existing fractures. *Proceedings of the SPE Unconventional Gas Recovery Symposium* (Soc Petrol Eng, Pittsburgh), pp 613–627.
23. Olson JE, Dahi-Taleghan A (2009) Modeling simultaneous growth of multiple hydraulic fractures and their interaction with natural fractures. *Proceedings of the SPE Hydraulic Fracturing Technology Conference* (Soc Petrol Eng, Pittsburgh).
24. Zeng X, Wei Y (2017) Crack deflection in brittle media with heterogeneous interfaces and its application in shale fracking. *J Mech Phys Solids* 101:235–249.
25. Bažant ZP, Oh BH (1983) Crack band theory for fracture of concrete. *Mater Constr* 16:155–177.
26. Červenka J, Bažant ZP, Wierer M (2005) Equivalent localization element for crack band approach to mesh-sensitivity in microplane model. *Int J Numer Methods Eng* 62:700–726.
27. Bazant ZP, Planas J (1997) *Fracture and Size Effect in Concrete and Other Quasibrittle Materials* (CRC Press, Boca Raton, FL), Vol 16.
28. Li C, Caner FC, Chau VT, Bažant ZP (2017) Spherocylindrical microplane constitutive model for shale and other anisotropic rocks. *J Mech Phys Sol* 103:155–178.
29. Hu DW, Zhou H, Zhang F, Shao J-F (2010) Evolution of poroelastic properties and permeability in damaged sandstone. *Int J Rock Mech Min Sci* 47:962–973.
30. Shojaei A, Taleghani AD, Li G (2014) A continuum damage failure model for hydraulic fracturing of porous rocks. *Int J Plast* 59:199–212.
31. Conil N, Djeran-Maigre I, Cabrillac R, Su K (2004) Poroplastic damage model for claystones. *Appl Clay Sci* 26:473–487.
32. Xie N, Zhu Q-Z, Shao J-F, Xu L-H (2012) Micromechanical analysis of damage in saturated quasi brittle materials. *Int J Solids Struct* 49:919–928.
33. Shao JF (1998) Poroelastic behaviour of brittle rock materials with anisotropic damage. *Mech Mater* 30:41–53.
34. Bažant ZP, Rahimi-Aghdam S (2016) Diffusion-controlled and creep-mitigated ASR damage via microplane model. I: Mass concrete. *J Eng Mech* 143:04016108.
35. Ortega JA, Ulm F-J, Abousleiman Y (2007) The effect of the nanogranular nature of shale on their poroelastic behavior. *Acta Geotech* 2:155–182.
36. Terzaghi K, Peck RB, Mesri G (1996) *Soil Mechanics in Engineering Practice* (John Wiley, New York).
37. Holtz RD, Kovacs WD (1981) *An Introduction to Geotechnical Engineering* (Prentice Hall, Englewood Cliffs, NJ).
38. Bažant Z, Jr. (1940) [Foundation breakdown behind sheetpiling wall]. *Technický Obzor*, p 132. Czech.
39. Bažant Z, Jr. (1953) [Stability of cohesionless soil in curvilinear upward seepage]. *SNTL Prague*, p 161. Czech.